

EFFECT OF THE PRANDTL NUMBER ON THE
CONVECTION FIELD AND THE HEAT TRANSFER
DURING NATURAL CONVECTION

B. M. Berkovskii and V. K. Polevikov

UDC 536.252

The spectrum of heat convective structures is analyzed over a wide range of the Prandtl number. An empirical formula is derived for determining, at any value of the Prandtl number, the range of the Rayleigh number within which the heat transfer and the temperature field can be described by the Rayleigh number alone.

During the last few years there has been published a great deal of material on theoretical and experimental studies as well as on numerical analysis of heat transfer during gravity convection in closed and laterally heated vessels. Several important questions have remained unanswered, however, among them the effect of the Prandtl number, of the Grashof number, and of the Rayleigh number on the convection process and on the heat transfer. Following a thorough analysis of the system of equations which describe heat convection, it has been established in [1] that at high values of the Rayleigh number (Ra) the dominant velocity and temperature gradients exist in the boundary layer and that, as the Rayleigh number increases, the thickness of this boundary layer decreases toward zero. It has also been shown there that within the central region of the cavity there forms a core of flow with a zero horizontal temperature gradient. G. Batchelor [1] has suggested that, as $Ra \rightarrow \infty$, this core becomes isothermal at the dimensionless temperature of $1/2$ and revolves with a finite constant vorticity which can be identified as the eigenvalue of the boundary-layer problem. After having solved this problem by the modified Fourier method, G. Poots [2] concurs with Batchelor's hypothesis. Experimental studies [1-8] and numerical analysis [8-14] of heat convection in closed and laterally heated vessels have confirmed Batchelor's and Poots' conclusions concerning the general trends in the development of heat convective structures. A great deal of study has been done concerning the core of flow which forms as the Rayleigh number increases. Most of the results confirm Batchelor's hypothesis about the core structure. It has been shown that, as $Ra \rightarrow \infty$, the vertical temperature gradient in the core does not vanish but, instead, stabilizes at some value which is too high to be disregarded. It has also been shown that the velocities in the core tend toward zero, as the Rayleigh number increases, which agrees with Batchelor's conclusions. Calculations made in [6-11] indicate that the heat transfer inside the cavity at a Prandtl number $Pr < 1$ depends on the Prandtl number as well as on the Rayleigh number, but only on the Rayleigh number when $Pr > 1$. These findings have made it feasible, at $Pr > 1$ and low values of the Grashof number, to solve the linearized system of equations which describes heat convection with only one governing parameter: the Rayleigh number.

We will note, however, that an experimental study of convective flow and heat transfer in a laterally heated cavity had to, for various reasons, yield very inaccurate results. Furthermore, the Rayleigh number in those tests was increased essentially by an increase in the Grashof number at 2 to 4 values of the Prandtl number. Owing to the lack of appropriate numerical methods, on the other hand, computations were made for insufficiently wide ranges of the modal parameters. There is a certain danger, therefore, of a strong bias in the discussion of results.

Recently finite-difference schemes have been developed which remain very stable as the values of the modal parameters increase, and this offers new possibilities for solving convection problems. The authors have tried to establish the effect of the Prandtl number and of other criterial groups on the convective

Institute of Heat and Mass Transfer, Academy of Sciences of the USSR, Minsk. Translated from *Inzhenerno-Fizicheskii Zhurnal*, Vol. 24, No. 5, pp. 842-849, May, 1973. Original article submitted June 30, 1972.

© 1975 Plenum Publishing Corporation, 227 West 17th Street, New York, N.Y. 10011. No part of this publication may be reproduced, stored in a retrieval system, or transmitted, in any form or by any means, electronic, mechanical, photocopying, microfilming, recording or otherwise, without written permission of the publisher. A copy of this article is available from the publisher for \$15.00.

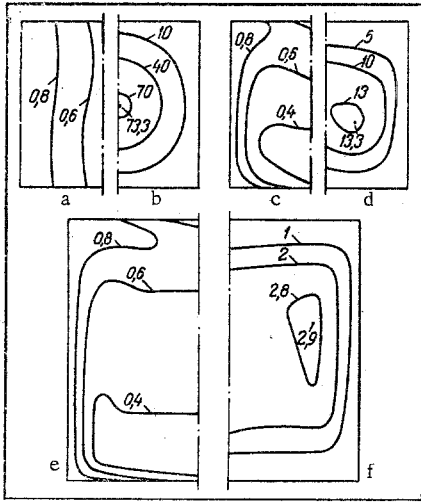


Fig. 1. Isotherms (a, c, e) and flow isolines (b, d, f) characterizing the development of heat convective structures within the low to medium range of the Prandtl number, with $Gr = 10^5$: a) and b) $Pr = 10^{-2}$, c) and d) $Pr = 1$, e) and f) $Pr = 10$; numbers next to the curves indicate the values of T and $-\psi$.

Here $T(x, y)$ denotes the temperature, $\omega(x, y)$ denotes the vorticity, $\psi(x, y)$ denotes the flow function, $u(x, y)$ and $v(x, y)$ denote the horizontal and the vertical velocity components, Pr is the Prandtl number, and Gr is the Grashof number.

The velocity components and the flow function are assumed zero at the region boundary:

$$u(x, y) = v(x, y) = \psi(x, y) = 0 \quad \text{at } x = 0, x = 1, y = 0, y = 1. \quad (1.2)$$

The boundary conditions for the temperature are stipulated as follows:

$$\begin{aligned} T(x, y) &= 1 & \text{at } x = 0; \\ T(x, y) &= 0 & \text{at } x = 1; \\ T(x, y) &= 1 - x & \text{at } y = 0, y = 1. \end{aligned} \quad (1.3)$$

2. System (1.1) with the boundary conditions (1.2) and (1.3) was solved numerically by the grid method. A second-order conservative monotonic finite-difference scheme was designed for this purpose, making use of concepts developed in [15, 16]. We note that each equation in system (1.1) is of the form

$$\frac{\partial}{\partial x} \left(m u \varphi - n \frac{\partial \varphi}{\partial x} \right) + \frac{\partial}{\partial y} \left(m v \varphi - n \frac{\partial \varphi}{\partial y} \right) = F, \quad (2.1)$$

where m and n are constants. The binomial $\partial/\partial x [m u \varphi - n(\partial \varphi/\partial x)] = [\partial f(x, y)/\partial x]$ was approximated by the balance method [16] as follows:

$$\begin{aligned} & \int_{x_{i-\frac{1}{2}}}^{x_{i+\frac{1}{2}}} \int_{y_{k-\frac{1}{2}}}^{y_{k+\frac{1}{2}}} \frac{\partial f(x, y)}{\partial x} dx dy = \left[\int_{y_{k-\frac{1}{2}}}^{y_{k+\frac{1}{2}}} f(x, y) dy \right]_{x_{i-\frac{1}{2}}}^{x_{i+\frac{1}{2}}} \\ & \approx h \left(m \varphi_{i+1, k} \frac{u_{i+\frac{1}{2}, k} - |u_{i+\frac{1}{2}, k}|}{2} + m \varphi_{i, k} \frac{u_{i+\frac{1}{2}, k} + |u_{i+\frac{1}{2}, k}|}{2} \right. \\ & \left. - \frac{2n^2}{2n + m |u_{i+\frac{1}{2}, k}| h} \cdot \frac{\varphi_{i+1, k} - \varphi_{i, k}}{h} - m \varphi_{i, k} \frac{u_{i-\frac{1}{2}, k} - |u_{i-\frac{1}{2}, k}|}{2} \right) \end{aligned}$$

structures and on the heat transfer during natural convection. We analyzed the problem of steady-state heat convection by gravity in a square cavity with lateral heating over a wide range of parameter values ($0 < Pr < 10^5$, $0 < Ra < 10^{10}$). The computations were made according to the second-order monotonic finite-difference scheme.

1. We consider a two-dimensional steady-state convective flow of a viscous incompressible fluid in a square region bounded by impermeable solid walls. We introduce Cartesian coordinates x, y with the origin at the lower left-hand corner of the square. The x -axis runs horizontally to the right, the y -axis runs vertically up. The system of dimensionless heat convection equations describing the steady state is then [14].

$$\begin{aligned} \frac{\partial \psi}{\partial y} \cdot \frac{\partial T}{\partial x} - \frac{\partial \psi}{\partial x} \cdot \frac{\partial T}{\partial y} &= \frac{1}{Pr} \left(\frac{\partial^2 T}{\partial x^2} + \frac{\partial^2 T}{\partial y^2} \right); \\ \frac{\partial \psi}{\partial y} \cdot \frac{\partial \omega}{\partial x} - \frac{\partial \psi}{\partial x} \cdot \frac{\partial \omega}{\partial y} &= \frac{\partial^2 \omega}{\partial x^2} + \frac{\partial^2 \omega}{\partial y^2} + Gr \frac{\partial T}{\partial x}; \\ \frac{\partial^2 \psi}{\partial x^2} + \frac{\partial^2 \psi}{\partial y^2} &= -\omega, \quad \left(\frac{\partial \psi}{\partial y} = u, \quad -\frac{\partial \psi}{\partial x} = v \right). \end{aligned} \quad (1.1)$$

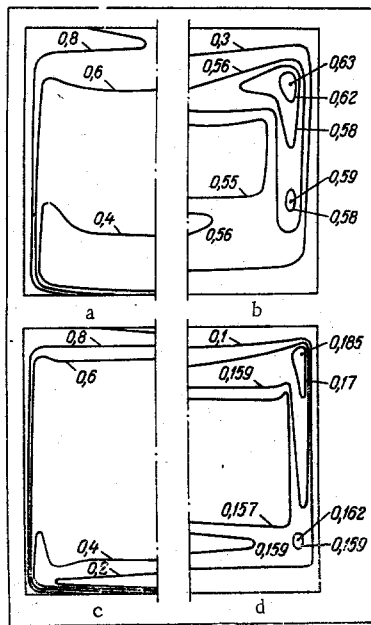


Fig. 2

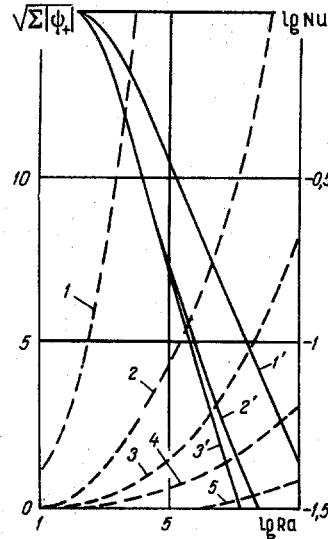


Fig. 3

Fig. 2. Isotherms (a, c) and flow isolines (b, d) characterizing the development of heat convective structures within the high range of the Prandtl number, with $Gr = 10^5$: a) and b) $Pr = 10^2$, c) and d) $Pr = 10^4$; numbers next to the curves indicate the values of T and $-\psi$.

Fig. 3. Effect of modal parameters on the convection rate and the heat transfer rate: 1) and 1') $Pr = 10^{-2}$, 2) and 2') $Pr = 1$, 3) and 3') $Pr = 10$, 4) $Pr = 10^2$, 5) $Pr = 10^4$.

$$-m\varphi_{i-1,k} \frac{u_{i-\frac{1}{2},k} + |u_{i-\frac{1}{2},k}|}{2} + \frac{2n^2}{2n+m|u_{i-\frac{1}{2},k}|h} \cdot \frac{\varphi_{i,k} - \varphi_{i-1,k}}{h}$$

and analogously the other functions and differential operators in (2.1). The difference analog of Eq. (2.1) can be written in the explicit form:

$$\varphi_{i,k} = (c_1\varphi_{i+1,k} + c_2\varphi_{i-1,k} + c_3\varphi_{i,k+1} + c_4\varphi_{i,k-1} + F_{i,k})/M, \quad (2.2)$$

where

$$c_1 = \frac{2n^2}{2n+m|u_{i+\frac{1}{2},k}|h} - mh \frac{u_{i+\frac{1}{2},k} - |u_{i+\frac{1}{2},k}|}{2},$$

$$c_2 = \frac{2n^2}{2n+m|u_{i-\frac{1}{2},k}|h} + mh \frac{u_{i-\frac{1}{2},k} + |u_{i-\frac{1}{2},k}|}{2},$$

$$c_3 = \frac{2n^2}{2n+m|v_{i,k+\frac{1}{2}}|h} - mh \frac{v_{i,k+\frac{1}{2}} - |v_{i,k+\frac{1}{2}}|}{2},$$

$$c_4 = \frac{2n^2}{2n+m|v_{i,k-\frac{1}{2}}|h} + mh \frac{v_{i,k-\frac{1}{2}} + |v_{i,k-\frac{1}{2}}|}{2},$$

$$M = \sum_i c_j.$$

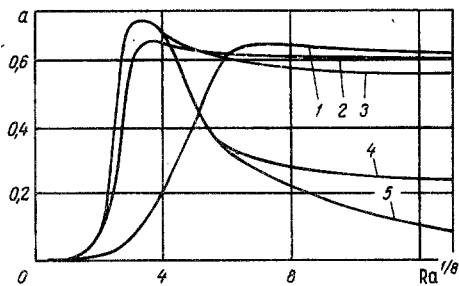


Fig. 4. Vertical temperature gradient in the core a , as a function of the modal parameters: 1) $Pr = 10^{-4}$, 2) 10^{-2} , 3) 1.0, 4) 10, 5) 10^2 .

We then used the averages

$$u_{i+\frac{1}{2},k} = \frac{\psi_{i+\frac{1}{2},k+\frac{1}{2}} - \psi_{i+\frac{1}{2},k-\frac{1}{2}}}{h} = \frac{\psi_{i,k+1} + \psi_{i+1,k+1} - \psi_{i,k-1} - \psi_{i+1,k-1}}{4h}$$

and analogously for

$$v_{i-\frac{1}{2},k}, v_{i,k+\frac{1}{2}}, v_{i,k-\frac{1}{2}}$$

Here we introduced a uniform spatial grid with h -steps. The function at the grid nodes was denoted by $\varphi_{i,k} = \varphi(ih, kh)$ where $i = 0, 1, 2, \dots, I$ and $k = 0, 1, 2, \dots, K$. The boundary conditions for the flow function and for the temperature in the difference form were put in the difference form:

$$\psi_{0,k} = \psi_{I,k} = \psi_{i,0} = \psi_{i,K} = 0; \quad (2.3)$$

$$T_{0,k} = 1, T_{I,k} = 0, T_{i,0} = T_{i,K} = 1 - ih.$$

The boundary conditions for the vorticity were determined approximately, with an accuracy $o(h^2)$, by expanding the flow function into Taylor series at points adjacent to the boundary and by taking into account Eqs. (1.1) with conditions (1.2). At $i = 0$ these boundary conditions were found to be

$$\omega_{0,k} = -\frac{8\psi_{1,k} - \psi_{2,k}}{2h^2}, \quad (2.4)$$

and analogously at the other boundaries.

The difference analog of system (1.1) was obtained according to scheme (2.2) with the boundary conditions (2.3)–(2.4) and then solved iteratively by the Euler method. In order to improve the convergence of the iteration process, we introduced relaxation parameters. As the first approximation we selected either the zero distribution of the function or the solution obtained for a different value of the modal parameter. The boundary values of vorticity (2.4) were computed after each iteration step.

The heat transfer through the cavity boundaries was characterized by the Nusselt number $Nu = (|Nu^+| + |Nu^-|)/2$. Here

$$|Nu^+| = \int_{\Gamma^+} \left(\frac{\partial T}{\partial n} \right)_{\Gamma^+} dl, \quad |Nu^-| = \int_{\Gamma^-} \left(\frac{\partial T}{\partial n} \right)_{\Gamma^-} dl, \quad (2.5)$$

with Γ^+ and Γ^- denoting the boundary segments with function $\partial T/\partial n$ respectively positive and negative. The derivative along the normal to the region boundary was approximated according to the second-order three-point formula. The integration in (2.5) was performed according to the Simpson formula.

In order to estimate the convection rate, we computed the quantity $\Sigma|\psi|$ representing the sum of local extrema of the difference function $|\psi_{i,k}|$ inside the square cavity.

The computations were made on a uniform 41×41 grid. For studying the convection with large velocity and temperature gradients, we also used a nonuniform 41×41 grid with steps varying from $1/80$ to $1/20$, depending on the magnitude of these gradients. A comparison of the results with control values obtained on uniform grids 21×21 and 31×31 confirmed the sufficiently high accuracy of the results. All operations were performed on a "Minsk-32" computer.

3. The effect of the Prandtl number on the development of convective structures and on the heat transfer at a fixed value of the Grashof number is shown in Fig. 1. Since the solution to the problem was found symmetric with respect to the center of the cavity, hence the isotherms and the flow isolines in one half of the square could be extrapolated into the entire region.

At low values of the Prandtl number (Fig. 1) the convection structure is unicellular and covers the entire region. The vortex center coincides with the cavity center. The streamlines here are almost concentric circles. The flow is uniform over the entire cell. The isotherms are almost straight lines parallel to the vertical edges. The horizontal temperature gradient in the cavity is approximately equal to unity, the vertical temperature gradient in the cavity is approximately equal to zero. As the Prandtl number increases, two vortices form at the center and move along the centerline of the square, each in the opposite direction. A closed boundary layer forms within which the dominant velocity and temperature fields are

concentrated. At the cavity center there forms a core of flow. The isotherms bend appreciably, especially at the ends. In the core region they become straight and horizontal, indicating that the horizontal temperature gradient inside the core decreases to zero.

At high values of the Prandtl number (Fig. 2) each vortex splits near the edges of the square into two new cells which, as the Prandtl number increases, separate from one another and move along the vertical edges toward the respective upper and lower corner. The larger of each pair tends toward the lower corner of the cavity at the hot edge and toward the upper corner of the cavity at the cold edge. The thickness of the boundary layer decreases, as $Pr \rightarrow \infty$, but slower than when the Grashof number increases at a fixed Prandtl number. The generated flow core expands appreciably. As the Prandtl number increases, the velocities here become negligibly lower than in the boundary layer. The temperature gradients in the boundary layer continue to increase and they increase faster than when $Gr \rightarrow \infty$.

An analysis of the curves in Fig. 3 will show how the convection rate and the heat transfer rate across the boundaries depend on the Prandtl number and on other governing parameters. At low values of the Prandtl number, heat is transmitted essentially by conduction. Convection is characterized here by a high flow velocity which, as $Pr \rightarrow 0$, approaches some constant limit and this limit is a function of the Grashof number. As the Prandtl number increases, convection takes over the major role in the heat transfer. The heat transfer rate across boundaries increases according to a power law. The convection rate tends to decrease to zero, as $Pr \rightarrow \infty$, while an increase in the Grashof number tends to increase the convection rate.

Of considerable interest are studies made of heat transfer and temperature fields in a closed cavity during a correlated variation in the governing parameters. Curves have been plotted in Fig. 4 which describe the trend of the vertical temperature gradient in the flow core under various convection modes. As the Rayleigh number increases, the vertical temperature gradient in the core increases up to its maximum value of approximately 0.6 to 0.7. At the same time, the rate of increase of this gradient is a function of the Prandtl number. As a result of the increase in the Rayleigh number, which follows an increase in the Prandtl number, the vertical temperature gradient in the core reaches its maximum and then monotonically decreases to zero. At the same time, as $Gr \rightarrow \infty$, this gradient stabilizes about a constant value which is a function of the Prandtl number and varies from 0 to 0.7. Thus, the core becomes isothermal when $Pr \rightarrow \infty$. An increase in the Grashof number results in a constant vertical temperature gradient too large to allow the core to be regarded as isothermal. In both cases there is almost no flow noted inside the core.

Calculations have shown that at certain critical values of the Rayleigh number (Ra_*) there occurs a sudden qualitative change in the development of heat transfer and in the temperature field structures. At subcritical values of the Rayleigh number the heat transfer rate and the temperature field are functions of the Rayleigh number alone. When $Ra > Ra_*$, however, then they become also functions of the Prandtl number. The points in Fig. 3 and 4 where the curves branch out correspond to the critical values of the Rayleigh number. It has been found that the critical Rayleigh number is a continuous and bilaterally unique function of the Prandtl number. The relation between both can be described approximately by the empirical formula

$$Ra_* = 10^{0.125(\lg Pr + 7)^2 - 1.125} \quad \text{for } 10^{-4} < Pr < 10^5. \quad (3.1)$$

The results obtained here lead to the following conclusion. For an arbitrary fixed value of the Prandtl number Pr_1 there exists such a critical Rayleigh number $Ra^*(Pr_1)$ determined according to formula (3.1) that in the range $Pr > Pr_1$ with $Ra < Ra^*$ the heat transfer rate and the temperature field can be described with a single parameter, namely the Rayleigh number. Consequently, at low values of the Prandtl number, the heat transfer rate and the temperature field are functions of the Rayleigh number within a very narrow range of low values of the Rayleigh number. At high values of the Prandtl number these process characteristics are determined by the Rayleigh number alone within a much wider range.

NOTATION

Ra	is the Rayleigh number;
Pr	is the Prandtl number;
x, y	are the space coordinates;
T	is the temperature;
ω	is the vorticity;

ψ is the flow function;
 u, v are the velocity components;
 Gr is the Grashof number;
 m, n are constants;
 φ is the universal designation for functions $T, \omega,$ and ψ ;
 $\varphi_{i,k}$ is the grid analog of function φ ;
 h is the grid step;
 Nu is the Nusselt number;
 n is the normal at the cavity boundary;
 Ra^* is the critical Rayleigh number.

LITERATURE CITED

1. G. Batchelor, *Quart. Appl. Mathem.*, 12, No. 3, 209 (1954).
2. G. Poots, *Quart. J. Mechan. and Appl. Mathem.*, 11, 257 (1958).
3. E. Eckert and W. Carlson, *Internatl. J. Heat and Mass Transfer*, 2, 106 (1961).
4. D. Dropkin and E. Somerscales, *Trans. ASME*, C87, No. 1 (1965).
5. J. Elder, *J. Fluid Mechan.*, 23, Part 1, 77 (1965).
6. A. Emery and N. Chu, *Trans. ASME*, C87, No. 1, 110 (1965).
7. R. MacGregor and A. Emery, *Trans. ASME*, C93, No. 2, 253 (1971).
8. R. MacGregor and A. Emery, *Trans. ASME*, C91, No. 3, 391 (1969).
9. G. DeVahl Davis, *Internatl. J. Heat and Mass Transfer*, 11, No. 11, 1675 (1968).
10. A. Rubel and F. Landis, *Phys. Fluids*, 12, No. 12, 11-208 (1969).
11. C. Quon, *Phys. Fluids*, 15, No. 1, 12 (1972).
12. J. Elder, *J. Fluid Mechan.*, 24, Part 4, 823 (1966).
13. G. DeVahl Davis and R. Thomas, *Phys. Fluids*, 12, No. 12, 11-198 (1969).
14. G. Z. Gershuni, E. M. Zhikhovitskii, and E. L. Tarunin, *Izv. Akad. Nauk SSSR Mekhan. Zidk. i Gaza*, No. 5, 56 (1966).
15. A. A. Samarskii, *Zh. Vychisl. Matem. i Matem. Fiz.*, 5, No. 3, 548 (1965).
16. A. A. Samarskii, *Introduction to the Theory of Difference Schemes [in Russian]*, Izd. Nauka, Moscow (1971).